

pubs.acs.org/joc Note

Cooperative Noncovalent Interactions Lead to a Highly Diastereoselective Sulfonyl-Directed Fluorination of Steroidal α,β -Unsaturated Hydrazones

Joseph N. Capilato, Maxime A. Siegler, Rozhin Rowshanpour, Travis Dudding,* and Thomas Lectka*



Cite This: J. Org. Chem. 2021, 86, 1300-1307



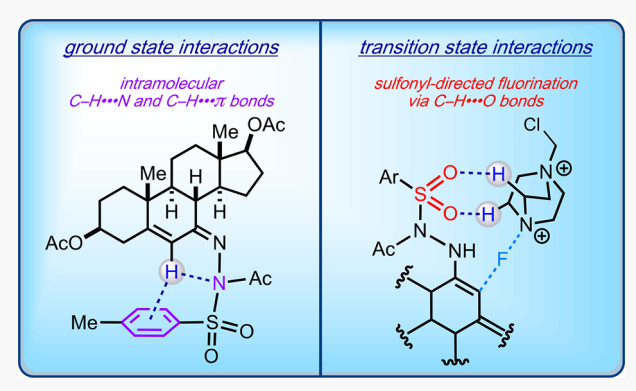
ACCESS I

III Metrics & More

Article Recommendations

S Supporting Information

ABSTRACT: A series of steroidal α,β -unsaturated hydrazones is presented whose behavior and reactivity are governed by various types of weak C–H hydrogen bonds. Several interesting features in a representative X-ray crystal structure and 1H NMR spectrum are examined that provide evidence for a unique bifurcated intramolecular C–H interaction. Moreover, these steroid derivatives undergo functionalization in the form of a highly regio- and stereoselective fluorination; the sulfonyl oxygen atoms are proposed to direct the fluorinating reagent through C–H hydrogen bonds.



Nonclassical hydrogen bonding, including C–H···n (n = lone pair) and C–H··· π bonds, has been the subject of increased attention in recent years. Of particular interest is the ability of such interactions to affect the structure and behavior of biological molecules, including proteins, lipids, and nucleic acids.1 For example, steroids, being principally hydrocarbonbased, may rely on $C-H\cdots\pi$ hydrogen bonds to form highly specific interactions with their corresponding receptor binding domains. One well-studied example of this can be seen in the binding of cholesterol to the β_2 -adrenergic receptor.³ Our laboratory, having experience in synthetic steroid chemistry, was interested in the potential to borrow this clever recognition paradigm from nature in order to address the synthetically challenging topic of stereoselectivity. In this note, we report steroid hydrazones that engage in putative C-H··· N/ π interactions in the ground state. However, a complementary set of C-H···O hydrogen bonds dictates a highly diastereoselective and apparently contrasteric sulfonyldirected fluorination in the transition state for the reaction with Selectfluor.

We began our studies with dehydroepiandrosterone (DHEA), an essential and abundant human steroid that is also utilized pharmaceutically under the name Prasterone. We reasoned that the oxidation of DHEA to the medicinally relevant enone would provide a suitable handle to functionalize the steroid skeleton with an aromatic moiety that had the proper orientation to stack intramolecularly on either the α - or β -face of the steroid. Thus, a concise synthesis of a diacetoxyenone derivative of DHEA was carried out according to our previously published protocol, followed by the

Scheme 1. Synthesis of Steroid Hydrazone 2 from DHEA

formation of the tosylhydrazone 1 (Scheme 1). While the hydrazone was successfully generated, we observed the partial solvolysis of the acetoxy esters under these conditions, likely due to the use of acidic methanol. Accordingly, another cycle of acylation produced compound 2, resulting from the unintentional (but serendipitous) acetylation of the sulfona-

Received: November 12, 2020 Published: December 10, 2020





mide to the sulfonimide. The 1H NMR spectrum of 2 contained some peculiar features, which complicated our identification of the compound; therefore, we obtained single-crystal X-ray diffraction data that allowed us to assign the structure unambiguously. Significantly, we observed two prominent intramolecular C–H interactions involving the vinylic C–H bond of the B-ring olefin: an apparently weak C–H···N hydrogen bond involving the hydrazino nitrogen atom and a C–H··· π interaction involving the aromatic ring (Figure 1). This π -interaction occurs on the α -face of the steroid

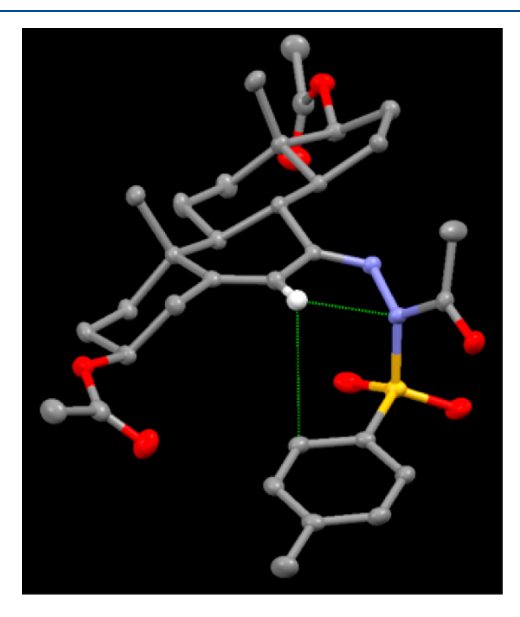


Figure 1. X-ray crystal structure of 2.

skeleton; the hydrazino moiety is oriented in such a fashion to enable both types of interactions, as the aryl ring adopts a quasi-slip-stacking (parallel-displaced) orientation below the Bring of the tetracycle. A short distance of 2.49 Å was measured from the C6 hydrogen atom to the acceptor nitrogen atom along with a C–H···N bond angle of 94°. Furthermore, a distance of 3.11 Å was measured from the hydrogen atom to the closest carbon atom in the phenyl ring of the tosyl group (C–H···C bond angle of ca. 114°); corroborating this interaction is pyrimidization of the nitrogen atom. Although these C–H···N/ π bond angles are relatively small, ¹⁰ this can be attributed at least in part to the bifurcated and intramolecular nature of the interaction.

To better understand this unique intramolecular interaction, we resynthesized the steroidal hydrazone 1, which was the originally intended target of this study. Performing the hydrazonation in neutral THF rather than acidic methanol allowed the straightforward isolation of 1 without the solvolysis of the acetoxy groups. Significantly, we observed a difference in the ¹H NMR of 1 compared to that of 2; the signal for the vinylic C–H bond of the B-ring olefin was abnormally broad and deshielded in steroid 2 (Figure 2). Given the crystal structure, we associate these spectroscopic features with the intramolecular C–H interactions in 2. The ¹H NMR spectrum of 1 is analogous to both the starting material DHEA and the enone derivative in that this signal is a sharp singlet rather than a broad one ¹¹ and is not unusually deshielded as it is in 2.

Next, we shifted focus to search for interesting reactivity. Noting that the intramolecular interaction occurs on the α -face of the steroid, we recognized this as a potential means to

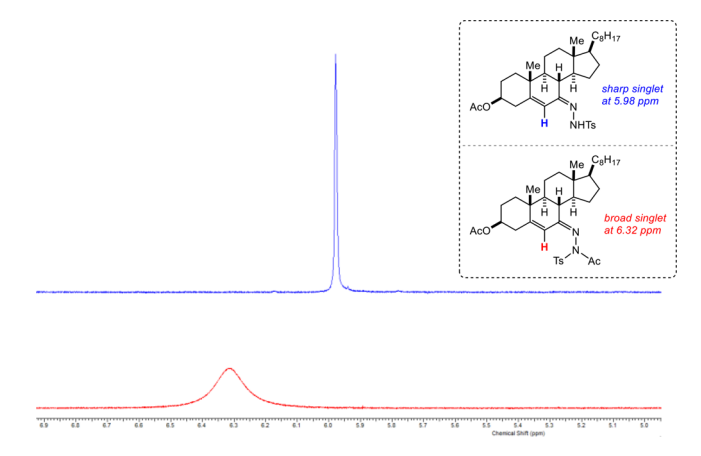


Figure 2. ¹H NMR comparison of vinylic C-H signals.

selectively functionalize the less-hindered β -face. Contributing to this goal, the hydrazone moiety itself is nucleophilic at the α -position through its enamine tautomer, ¹² meaning that potential functionalizations could benefit from being site-selective in addition to stereoselective. In the case of α , β -unsaturated hydrazone 2, we anticipated the formation of a dienamine with a nucleophilic character at the C4 position of the steroid's A-ring. Surprisingly, such functionalizations of steroid imines are scant in the literature, although several examples have been reported using these precursors to access steroid lactams or amines by either a Beckman rearrangement or a reduction, respectively. ¹³

Given our interest in the fluorination of steroids, we subjected cholesterol hydrazone 4 to a simple reaction with Selectfluor. A high-yield fluorination occurred that was both regio- and stereoselective, affording product 8 in a 76% yield (Scheme 2). The reaction proceeds under mild conditions—it

Scheme 2. Fluorination of Steroid Hydrazone 4

is nonphotochemical and uncatalyzed—and occurs at room temperature in the dark. In regard to the site-selectivity, the fluorine atom was established to be at C6 (B-ring, α -position to the imine) rather than the initially proposed C4 position on the A-ring. This discrepancy is interesting as we first anticipated the reaction of the dienamine intermediate at C4 to reestablish the α , β -unsaturated imine rather than the formation of the allylic ester. The facial selectivity of the fluorination is also counterintuitive at first glance; the reaction occurs on the α -face of the steroid rather than the putatively less-hindered β -face.

Another interesting feature of product 8 is the loss of the acetamide group, as the typically stable sulfonimide was cloven to the sulfonamide during fluorination. To gain insight into this unusual occurrence, we subjected hydrazone 4h (which lacks the sulfonimide) to a fluorination under the same conditions. Surprisingly, the reaction did not take place with

this derivative, further demonstrating the unique reactivity of steroid 4. To follow up on this result, we synthesized an N-methyl analogue, 9, to probe the necessity of the acetimide group (Figure S21).¹⁴ This steroid was subjected to the fluorination and was found to undergo the reaction in identical regio- and stereoselectivities to the imide hydrazones, albeit in a lower yield (ca. 30%).¹⁵

To improve the synthetic utility of the fluorination, we considered methods to remove the hydrazone group under mild conditions, which would be necessary to make medicinally relevant fluorosteroids. While several options exist to accomplish this goal, including Wolff—Kishner-type reactions, we stumbled across a simpler solution. We found that adding a small portion of additional Selectfluor to the reaction mixture after fluorination resulted in the apparent hydrolysis of the hydrazone products to the corresponding ketone in a one-pot fashion. Synthetically, this becomes advantageous as one can toggle between fluorinated hydrazone or ketone products simply by controlling the stoichiometry of the Selectfluor.

We next sought to determine whether other steroids could participate in this unique C–H interaction and fluorination. Conveniently, the B-ring olefin found in DHEA is conserved across many naturally occurring steroids (Δ^5 -steroids), ¹⁹ enabling synthesis of a variety of derivatives using analogous methods. A cholesterol hydrazone was prepared ²⁰ (compound 4) using the synthesis outlined for steroid 2 (Figure 3). This

substrate	product	yield
2 Me H H H H N N AcTos	3 Me H H H H H	58%
Me, Me Me, Me Me, Me NAcTos	Me,	∕ -Ме
6 Me H H H H Aco	7 Me H H H H H H	61%

Figure 3. Product examples for hydrazone fluorination.

steroid engages in both the C–H interactions and the fluorination, delivering product 5 despite a substantial difference in the D-ring substituent. Along these lines, the spiroketal steroid diosgenin²¹ was employed to synthesize a hydrazone analogue, 6, that was found to undergo the C–H interactions and the fluorination, giving fluoride 7.

Originally, we proposed that steric effects should control the stereoselectivity of the reaction. Given the observed C–H interactions described above, the tosylhydrazone moiety is positioned toward the α -face of the steroid, resulting in the β -

face experiencing noticeably less steric hindrance. As noted, we found that the fluorination exclusively produced the α -fluoride product. Further complicating our analysis was the literature precedent for the fluorination of steroids at the same position (C6). Rozatian et al. reported a 43:57 mixture of diastereomers for C6 fluorination of a steroid enol ester using Selectfluor (Figure 4).²² On the other hand, higher β -selectivity was

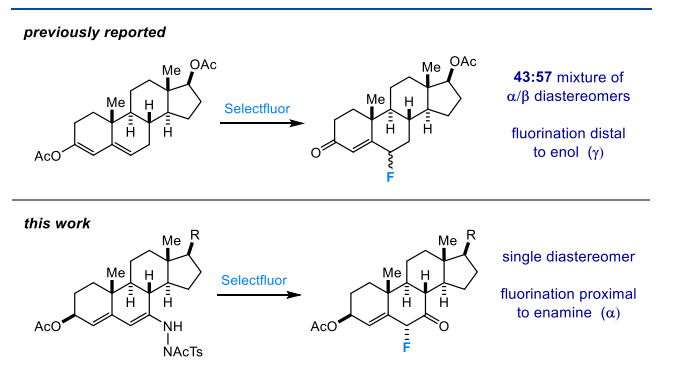


Figure 4. Literature precedent for fluorination at C6.

observed using bulky boron complexing agents. ²³ Moreover, the fluorination in these examples occurred distal (γ) to the enol to regenerate the conjugated enone, in contrast to our results.

To explain these observations, along with the finding that fluorination occurred on the more hindered face of the steroid, we propose that the sulfonylhydrazone moiety acts as a directing group. Recently, we reported the mechanistic study of a regioselective radical-based fluorination of steroids and other complex substrates. To our surprise, the selectivity of this reaction was driven by the ability of the Selectfluor-based radical cation to hydrogen bond to a carbonyl group on the substrate.²⁴ In the present reaction, we propose that the oxygen atoms of the sulfonyl group may be operating analogously to those carbonyls (acting as a hydrogen bond acceptor to the relatively acidic hydrogen atoms found in Selectfluor).

We turned to computational chemistry to examine the transition state for fluorination. The literature precedent for electronically similar enol esters suggests that a two-electron process may be occuring.²⁵ Couple this with our stereochemical data, which is difficult to reconcile with outer-sphere one-electron chemistry, and we chose to focus on the possibility of a concerted transition state, bearing in mind that the synchronicity of electron transfer could vary. Emerging from these calculations was a preferred α -fluorination transition state α -TS1 $_{\alpha}$ with a Gibbs free-energy activation barrier of 16.0 kcal/mol relative to the reacting components (Figure 5, calculated at ω b97xd/6-31G(d,p)// ω B97Xd/6-311+G(d,p) (MeCN)). Structurally, a hydrogen bond network defines the transition state, steering the fluorination to the α face of the steroid substrate. Crucial to this network is a twopoint hydrogen bond interaction with distances of 2.15 and 2.29 Å acting as a directing group tether between both sulfonyl oxygen atoms and two Selectfluor hydrogen atoms adjacent to the bridgehead nitrogen engaged in fluorine transfer. In addition, a pair of stabilizing hydrogen bonds with distances of 2.20 and 2.36 Å bridges the acetoxy carbonyl oxygen to the two hydrogen atoms of Selectfluor. A carbon-fluorine bondforming distance of 2.20 Å and a nitrogen-fluoride bondbreaking distance of 1.59 Å were measured. Lastly, the role of

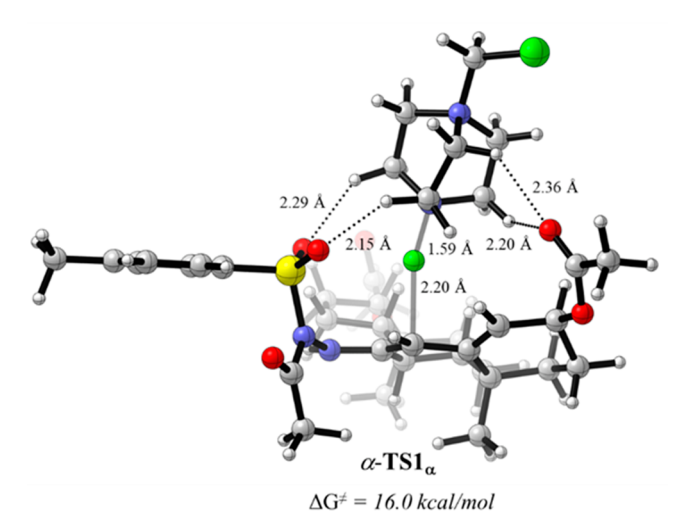


Figure 5. Computed transition state for the fluorination of 2.

Coulombic charge stabilization is notable as seen in the molecular electrostatic potential map (MEP) surface (Figure S29, left-hand side), wherein the electronegative sulfonyl and acetoxy group (red) reach out like guiding hands to direct Selectfluor (blue).

In contrast, the β -fluorination transition state α -TS1 $_{\beta}$, with an activation barrier of 17.5 kcal/mol, was disfavored despite having bond-making and bond-breaking distances similar to those of α -TS1 $_{\alpha}$ as well as a hydrogen bond network (Figure S29). Diving deeper into this structure nevertheless reveals the slippage of the anchoring and strongly directing sulfonyl group two-point hydrogen bond of α -TS1 $_{\alpha}$. Furthering the stereoselective preference, the sulfonyl groups are inherently oriented toward the α -face given the C–H···N/ π interaction, and this fact explains the apparent paradox of contrasteric reactivity.

On the other hand, γ -fluorination of the enamine is uncompetitive, with relative Gibbs free activation barriers in excess of 24 kcal/mol. In this case, disrupting the stabilizing sulfonyl hydrogen bonding resulted in γ -fluorination being disfavored (see the Supporting Information for α - and β -face γ -fluorination transition states γ -TS1 $_{\alpha}$ and γ -TS1 $_{\beta}$, respectively).

Given the unique role of Selectfluor in this particular fluorination, we became interested in testing an alternative electrophilic fluorinating reagent in the reaction. We proposed that structurally distinct fluorinating reagents might deliver the same fluoride product, albeit without the stereoselectivity that is observed with Selectfluor. Steroid **2** was subjected to a reaction with *N*-fluorobenzenesulfonimide (NFSI); however, no fluorination occurred at room temperature, and NFSI only reacted upon heating. Several trace fluorinated products were formed, although none resembled the products obtained with Selectfluor. As NFSI is often interchangeable with Selectfluor in simple electrophilic fluorinations,²⁷ this experiment highlights the unique reactivity of Selectfluor in certain cases.

In conclusion, we have developed a diastereoselective fluorination of steroid α,β -unsaturated hydrazones. Sulfonyl directing groups are shown to hydrogen bond to C–H atoms on the fluorination reagent in the transition state. In the ground state, however, these steroids experience an intramolecular bifurcated C–H···N/ π interaction. This work demonstrates once again the powerful cumulative effects of

relatively weak interactions, such as C-H hydrogen bonds, on stereoselectivity.

■ EXPERIMENTAL SECTION

General Information. Unless otherwise stated, all reactions were carried out under strictly anhydrous conditions and a N_2 atmosphere. All solvents were dried and distilled by standard methods. All 1 H spectra were acquired on a 400 MHz NMR spectrometer in CDCl₃, 19 F spectra were acquired on a 300 MHz NMR spectrometer in CD₃CN or CDCl₃, and 13 C NMR spectra were acquired on a 400 MHz NMR spectrometer in CDCl₃. The 1 H, 13 C, and 19 F NMR chemical shifts are given in parts per million (δ) with respect to an internal tetramethylsilane (TMS, δ = 0.00 ppm) standard or 3-chlorobenzotrifluoride (δ = -64.2 ppm relative to CFCl₃). NMR data are reported in the following format: chemical shift (integration, multiplicity (s = singlet, d = doublet, t = triplet, q = quartet, m = multiplet), coupling constants (Hertz)).

General Fluorination Procedure. The substrate (1.0 mmol) was added to an oven-dried round-bottom flask equipped with a stir bar and then dissolved in anhydrous acetonitrile (20 mL). Selectfluor (2.0 mmol, 2.0 equiv) was added, and the reaction mixture stirred at room temperature overnight (12–24 h) and was monitored by ¹⁹F NMR. For the ketone products, an additional 1.0 equiv of Selectfluor was added after the fluorination transpired, and the reaction mixture was stirred for 2–4 h. The reaction was quenched with 1 M HCl (50 mL), and the reaction mixture was transferred to a separatory funnel, diluted with H₂O, and extracted into CH₂Cl₂ (3×). The combined organic layers were washed with brine, dried with Na₂SO₄, and concentrated to dryness. The crude reaction mixture was purified via gradient column chromatography on silica gel with EtOAc/hexanes.

Fluorinated Product Characterization Data. Compound 3. Fluorination was run according to the general procedure, and the product was isolated via gradient column chromatography on silica gel with EtOAc/hexanes: white solid (236 mg, 58%); ¹⁹F NMR (282 MHz, CDCl₃) δ –203.70 (d, J = 48.2 Hz); ¹H NMR (400 MHz, CDCl₃) δ 5.73 –5.69 (1H, m), 5.51 –5.33 (1H, m), 5.30 –5.22 (1H, m), 4.65 (1H, t, J = 8.7 Hz), 2.47 (1H, t, J = 11.6 Hz), 2.28 –2.18 (2H, m), 2.06 (3H, s), 2.05 –2.02 (4H, m), 1.89 –1.73 (2H, m), 1.59 –1.42 (4H, m), 1.34 (3H, s), 1.28 –1.09 (4H, m), 0.94 –0.76 (4H, m); ¹³C [¹H]NMR (100 MHz, CDCl₃) δ 202.6 (d, ² J_{C-F} = 13.9 Hz), 171.0, 170.5, 143.0 (d, ³ J_{C-F} = 11.4 Hz), 119.6 (d, ² J_{C-F} = 1.5 Hz), 53.3, 47.2, 43.3 (d, ⁴ J_{C-F} = 1.8 Hz), 42.4, 37.7 (d, ⁴ J_{C-F} = 2.9 Hz), 35.5, 35.1 (d, ⁴ J_{C-F} = 1.1 Hz), 27.5, 24.7, 24.0, 21.2, 21.1, 20.8, 19.0, 12.1; HRMS (ESI-Orbitrap) m/z [M + H]⁺ calcd for C₂₃H₃₂O₅F⁺ 407.2235, found 407.2224.

Compound 5. Fluorination was run according to the general procedure, and the product was isolated via gradient column chromatography on silica gel with EtOAc/hexanes: white solid (331 mg, 72%); ¹⁹F NMR (282 MHz, CDCl₃) δ –203.44 (d, J = 48.8 Hz); ¹H NMR (400 MHz, CDCl₃) δ 5.71–5.68 (1H, m), 5.49–5.33 (1H, m), 5.30–5.23 (1H, m), 2.41 (1H, t, J = 11.7 Hz), 2.24–2.14 (1H, m), 2.09–2.00 (5H, m), 1.96–1.89 (1H, m), 1.87–1.80 (1H, m), 1.56–1.40 (5H, m), 1.36–1.31 (5H, m), 1.21–1.07 (7H, m), 1.05–0.89 (6H, m), 0.88–0.85 (7H, m), 0.68 (3H, s); ¹³C{¹H}NMR (100 MHz, CDCl₃) δ 203.3 (d, ²J_{C-F} = 13.9 Hz), 170.6, 143.5 (d, ³J_{C-F} = 11.4 Hz), 119.2 (d, ²J_{C-F} = 14.3 Hz), 91.7 (C–F, d, ¹J_{C-F} = 198.8 Hz), 69.9 (d, ⁴J_{C-F} = 1.1 Hz), 54.9, 53.4, 48.2 (d, ⁴J_{C-F} = 1.5 Hz), 47.5, 42.4, 39.4, 38.3, 37.7 (d, ⁴J_{C-F} = 2.9 Hz), 36.1, 35.6, 35.1 (d, ⁴J_{C-F} = 1.1 Hz), 28.3, 28.0, 24.7, 24.5, 23.7, 22.8, 22.5, 21.3, 21.2, 19.0, 18.7, 12.0; HRMS (ESI-Orbitrap) m/z [M + H]⁺ calcd for C₂₉H₄₆O₃F⁺ 461.3432, found 461.3421.

Compound 7. Fluorination was run according to the general procedure, and the product was isolated via gradient column chromatography on silica gel with EtOAc/hexanes: white solid (298 mg, 61%); ¹⁹F NMR (282 MHz, CDCl₃) δ –203.53 (d, J = 48.8 Hz); ¹H NMR (400 MHz, CDCl₃) δ 5.73–5.68 (1H, m), 5.52–5.35 (1H, m), 5.29–5.22 (1H, m), 4.54–4.45 (1H, m), 3.50–3.44 (1H, m), 3.37 (1H, t, J = 10.9 Hz), 2.63–2.54 (2H, m), 2.09–2.03 (4H, m),

 $1.86-1.72~(4\rm H,\ m),\ 1.64-1.59~(3\rm H,\ m),\ 1.56~(3\rm H,\ s),\ 1.51-1.38~(3\rm H,\ m),\ 1.35~(3\rm H,\ s),\ 1.24-1.11~(4\rm H,\ m),\ 0.98~(3\rm H,\ d,\ J=6.9~Hz),\ 0.81-0.76~(6\rm H,\ m);\ ^{13}C\{^{1}\rm H\}NMR~(100~MHz,\ CDCl_3)~\delta~202.7~(d,\ ^{2}\!\!J_{\rm C-F}=13.9~Hz),\ 170.6,\ 143.1~(d,\ ^{3}\!\!J_{\rm C-F}=11.4~Hz),\ 119.5~(d,\ ^{2}\!\!J_{\rm C-F}=13.9~Hz),\ 109.3,\ 91.7~(C-F,\ d,\ ^{1}\!\!J_{\rm C-F}=199.2~Hz),\ 80.6,\ 69.8~(d,\ ^{4}\!\!J_{\rm C-F}=1.1~Hz),\ 66.8,\ 61.1,\ 53.3,\ 47.8~(d,\ ^{4}\!\!J_{\rm C-F}=1.5~Hz),\ 46.8,\ 41.5,\ 40.2,\ 38.3,\ 37.7~(d,\ ^{4}\!\!J_{\rm C-F}=2.9~Hz),\ 35.1,\ 31.8,\ 31.4,\ 30.3,\ 28.8,\ 24.7,\ 21.2,\ 21.0,\ 19.0,\ 17.1,\ 16.4,\ 14.5;\ HRMS~(ESI-Orbitrap)~m/z~[M~+~H]^+~calcd~for~C_{29}H_{42}O_5F^+~489.3017,~found~489.3008.$

Compound 8. Fluorination was run according to the general procedure (quenched with saturated aq. NaHCO3 instead of HCl and using 1.5-2.0 equiv Selectfluor), and the product was isolated via gradient column chromatography on silica gel with EtOAc/hexanes: white solid (478 mg, 76%); 19 F NMR (282 MHz, CDCl₃) δ –189.28 (d, J = 47.6 Hz); ¹H NMR (400 MHz, CDCl₃) δ 7.87–7.83 (2H, m), 7.33-7.29 (2H, m), 5.73-5.45 (2H, m), 5.35-5.27 (1H, m), 2.48-2.39 (4H, m), 2.29-2.19 (2H, m), 2.11-2.00 (6H, m), 1.87-1.74 (2H, m), 1.67-1.48 (5H, m), 1.40-1.24 (6H, m), 1.21 (3H, s), 1.18-1.08 (5H, m), 0.93 (3H, d, J = 6.5 Hz), 0.89-0.86 (6H, m), 0.71 (3H, s); ${}^{13}C\{{}^{1}H\}NMR$ (100 MHz, CDCl₃) δ 170.5, 167.7, 144.8, 142.9 (d, ${}^{3}J_{C-F} = 12.8 \text{ Hz}$), 135.3, 129.4, 128.5, 121.7 (d, ${}^{2}J_{C-F}$ = 15.8 Hz), 90.7 (C–F, d, ${}^{1}J_{C-F}$ = 201.0 Hz), 70.0, 55.1, 50.0, 43.8, 42.7, 39.5, 38.3, 37.4 (d, ${}^{4}J_{C-F}$ = 2.6 Hz), 36.1, 35.6, 35.1, 28.1, 28.0, 24.9, 24.6, 24.3, 23.7, 22.8, 22.5, 21.6, 21.2, 21.0, 19.1, 18.8, 12.0; HRMS (ESI-Orbitrap) m/z [M + H]⁺ calcd for $C_{36}H_{54}O_4N_2FS^+$ 629.3789, found 629.3806.

Syntheses and Characterization of Starting Materials. Compound 2. Dehydroepiandrosterone (2.5 g, 8.67 mmol) was dissolved in MeOH (55 mL), and the mixture was cooled to 0 $^{\circ}$ C in an ice bath. Sodium borohydride (410 mg, 10.84 mmol, 1.25 equiv) was added in three portions. The mixture was stirred at 0 $^{\circ}$ C for an additional 30 min and then slowly warmed to room temperature, where it continued to stir for 4 h. The reaction was quenched with 1 M HCl (25 mL), and then most of the MeOH was removed in vacuo. The precipitate was filtered, washed with water, and dried overnight under vacuum.

The crude solid was suspended in pyridine (10 mL); cat. DMAP was added (50 mg), then acetic anhydride (7 mL) was added dropwise. The mixture was heated at 95 $^{\circ}$ C for 24 h with a heating mantle. After cooling to room temperature, the reaction was quenched with water (150 mL), and the resulting precipitate was filtered and washed with water. This solid was then dissolved with DCM (100 mL) and washed in a separatory funnel with 1 M HCl, followed by brine. The solvent was dried over Na₂SO₄ and then concentrated to dryness.

The crude material from the previous step (8.5 mmol) was dissolved in acetone (140 mL). N-Hydroxysuccinimide (2.93 g, 25.5 mmol, 3.0 equiv) was added, followed by $K_2Cr_2O_7$ (10.0 g, 34 mmol, 4.0 equiv) and glacial acetic acid (14 mL). The mixture was stirred at 50 °C for 48 h with a heating mantle and then cooled to room temperature. The mixture was diluted with Et_2O and filtered through Celite (washed with Et_2O). Most of the acetone was removed in vacuo, and the mixture was diluted with more Et_2O and washed with water, then saturated sodium bicarbonate, and finally brine. The organic layer was dried over Na_2SO_4 , concentrated to dryness, and then purified via column chromatography on silica gel (EtOAc/hexanes), providing the diacetoxy enone of DHEA as a white solid (2.1 g, 62% from DHEA).

The product from the previous step (2.1 g, 5.4 mmol) was dissolved in anhydrous THF (60 mL). Tosyl hydrazide (2.51 g, 13.5 mmol, 2.5 equiv) was added, and the mixture was refluxed for 24 h with a heating mantle. After cooling to room temperature, the reaction mixture was diluted with EtOAc and washed with saturated sodium bicarbonate, followed by brine. The organic layer was dried over Na₂SO₄, concentrated to dryness, and purified via column chromatography on silica gel (EtOAc/hexanes), providing the hydrazone of DHEA as a white solid (2.3 g, 78%).

The hydrazone from the previous step (2.3 g, 4.2 mmol) was dissolved in CH₂Cl₂. Et₃N (1.2 mL, 8.4 mmol, 2.0 equiv) and cat. DMAP (0.1 equiv) were added, followed by acetic anhydride

dropwise (0.8 mL, 8.4 mmol, 2.0 equiv). The reaction mixture was stirred overnight at room temperature, then was diluted with more DCM and transferred to a separatory funnel. The solution was washed with saturated sodium bicarbonate, followed by brine. The organic layer was then dried over Na₂SO₄ and concentrated to dryness. Purification via column chromatography on silica gel (EtOAc/ hexanes) provided compound 2 as a white solid (2.1 g, 86%): ¹H NMR (400 MHz, CDCl₃) δ 7.88–7.84 (2H, m), 7.35–7.31 (2H, m), 6.34 (1H, br. s), 4.76-4.59 (2H, m), 2.67-2.47 (3H, m), 2.44 (3H, s), 2.42-2.33 (1H, m), 2.22-2.11 (1H, m), 2.06 (3H, s), 2.05 (3H, s), 2.04 (3H, s), 2.02-1.91 (2H, m), 1.83-1.75 (1H, m), 1.71-1.40 (8H, m), 1.30-1.23 (1H, m), 1.21 (3H, s), 0.86 (3H, s); ¹³C{¹H}-NMR (100 MHz, CDCl₃) δ 180.0, 171.2, 170.1, 169.4, 160.0, 144.9, 135.2, 129.4, 128.7, 116.7, 81.9, 72.3, 48.9, 44.9, 42.7, 40.4, 39.0, 38.2, 36.1, 35.3, 27.3, 27.2, 27.0, 24.4, 21.7, 21.2, 21.1, 20.3, 17.6, 12.2; HRMS (ESI-Orbitrap) m/z [M + H]⁺ calcd for $C_{32}H_{43}O_7N_2S^+$ 599.2792, found 599.2782.

Compound 4. Cholesterol (2.5 g, 6.47 mmol) was dissolved in CH_2Cl_2 . Et_3N (1.8 mL, 12.94 mmol, 2.0 equiv) and cat. DMAP (0.1 equiv) were added, followed by acetic anhydride dropwise (1.22 mL, 12.94 mmol, 2.0 equiv). The reaction mixture was stirred overnight at room temperature, then diluted with more DCM and transferred to a separatory funnel. The solution was washed with 1 M HCl, then saturated sodium bicarbonate, and finally brine. The organic layer was then dried over Na_2SO_4 and concentrated to dryness.

The crude material from the previous step (6.4 mmol) was dissolved in acetone (105 mL). N-Hydroxysuccinimide (2.21 g, 19.2 mmol, 3.0 equiv) was added, followed by $K_2Cr_2O_7$ (7.53 g, 25.6 mmol, 4.0 equiv) and glacial acetic acid (10.5 mL). The mixture was stirred at 50 °C for 48 h with a heating mantle, then cooled to room temperature. The mixture was diluted with Et_2O and filtered through Celite (washed with Et_2O). Most of the acetone was removed in vacuo, and the mixture was diluted with more Et_2O and washed with water, then saturated sodium bicarbonate, and finally brine. The organic layer was dried over Na_2SO_4 , concentrated to dryness, and purified via column chromatography on silica gel (EtOAc/hexanes), providing the acetoxy enone of cholesterol as a white solid (2.03 g, 71% from cholesterol).

The product from the previous step (2.03 g, 4.59 mmol) was dissolved in anhydrous THF (51 mL). Tosyl hydrazide (2.14 g, 11.475 mmol, 2.5 equiv) was added, and the mixture was refluxed for 24 h with a heating mantle. After cooling to room temperature, the reaction was diluted with EtOAc and washed with saturated sodium bicarbonate, followed by brine. The organic layer was dried over Na₂SO₄, concentrated to dryness, and purified via column chromatography on silica gel (EtOAc/hexanes), providing the hydrazone of DHEA as a white solid (1.91 g, 68%).

The hydrazone from the previous step (1.91 g, 3.12 mmol) was dissolved in CH₂Cl₂. Et₃N (0.87 mL, 6.24 mmol, 2.0 equiv) and cat. DMAP (0.1 equiv) were added, followed by acetic anhydride dropwise (0.6 mL, 6.24 mmol, 2.0 equiv). The reaction mixture stirred overnight at room temperature, then diluted with more DCM and transferred to a separatory funnel. The solution was washed with saturated sodium bicarbonate and brine. The organic layer was dried over Na₂SO₄ and concentrated to dryness. Purification via column chromatography on silica gel (EtOAc/hexanes) provided compound 4 as a white solid (1.67 g, 82%): 1 H NMR (400 MHz, CDCl₃) δ 7.88-7.85 (2H, m), 7.32-7.29 (2H, m), 6.32 (1H, br. s), 4.74-4.64 (1H, m), 2.59-2.44 (3H, m), 2.41 (3H, s), 2.40-2.33 (1H, m), 2.03 (3H, s), 2.00 (3H, s), 1.99-1.88 (2H, m), 1.86-1.77 (1H, m), 1.70-1.46 (6H, m), 1.39–1.21 (5H, m), 1.19–1.07 (9H, m), 0.95–0.91 (3H, m), 0.87-0.84 (6H, m), 0.83-0.74 (2H, m), 0.71 (3H, s); 13 C{ 1 H}NMR (100 MHz, CDCl₃) δ 180.6, 170.0, 169.5, 159.5, 144.7, 135.3, 129.2, 128.7, 116.8, 72.4, 54.6, 50.0, 42.8, 40.7, 39.4, 38.9, 38.1, 38.0, 36.1, 35.5, 28.2, 27.9, 27.3, 27.2, 26.8, 24.3, 23.7, 22.7, 22.5, 21.6, 21.1, 20.7, 18.9, 17.4, 12.0; HRMS (ESI-Orbitrap) m/z [M + H]⁺ calcd for $C_{38}H_{57}O_5N_2S^+$ 653.3989, found 653.3974.

Compound 6. Diosgenin (2.5 g, 6.03 mmol) was dissolved in CH₂Cl₂. Et₃N (1.7 mL, 12.06 mmol, 2.0 equiv) and cat. DMAP (0.1 equiv) were added, followed by acetic anhydride dropwise (1.14 mL,

12.06 mmol, 2.0 equiv). The reaction mixture was stirred overnight at room temperature, then was diluted with more DCM and transferred to a separatory funnel. The solution was washed with saturated sodium bicarbonate and then brine. The organic layer was then dried over Na_2SO_4 and concentrated to dryness.

The crude material from the previous step (6.0 mmol) was dissolved in EtOAc (50 mL), and 3 Å activated molecular sieves were added (2.0 g). tert-Butyl hydroperoxide in decane (5.48 mL, 5.0 equiv) was added. After stirring for 5–10 min, Mn(OAc)₃ was added (186 mg, 0.1 equiv), and the reaction mixture was stirred for 24 h at room temperature. The mixture was filtered through Celite and concentrated to dryness. Purification via column chromatography on silica gel (EtOAc/hexanes) provided the enone as a white solid (2.07 g, 73% from diosgenin).

The product from the previous step (2.07 g, 4.4 mmol) was dissolved in anhydrous THF (50 mL). Tosyl hydrazide (2.05 g, 11.0 mmol, 2.5 equiv) was added, and the mixture was refluxed for 24 h with a heating mantle. After cooling to room temperature, the reaction was diluted with EtOAc and washed with saturated sodium bicarbonate, followed by brine. The organic layer was dried over Na₂SO₄, concentrated to dryness, and purified via column chromatography on silica gel (EtOAc/hexanes), providing the hydrazone of diosgenin as a white solid (1.80 g, 64%).

The hydrazone from the previous step (1.80 g, 2.82 mmol) was dissolved in CH₂Cl₂. Et₃N (0.79 mL, 5.64 mmol, 2.0 equiv) and cat. DMAP (0.1 equiv) were added, followed by acetic anhydride dropwise (0.53 mL, 5.64 mmol, 2.0 equiv). The reaction mixture was stirred overnight at room temperature, then was diluted with more DCM and transferred to a separatory funnel. The solution was washed with saturated sodium bicarbonate and then brine. The organic layer was dried over Na2SO4 and concentrated to dryness. Purification via column chromatography on silica gel (EtOAc/ hexanes) provided compound 6 as a white solid (1.69 g, 88%): ¹H NMR (400 MHz, CDCl₃) δ 7.88–7.84 (2H, m), 7.35–7.31 (2H, m), 6.32 (1H, br. s), 4.76–4.66 (1H, m), 4.43 (1H, q, J = 7.6 Hz), 3.52– 3.45 (1H, m), 3.38 (1H, t, J = 11.0 Hz), 2.85–2.78 (1H, m), 2.75– 2.64 (1H, m), 2.59-2.53 (1H, m), 2.51-2.46 (1H, m), 2.43 (3H, s), 2.04 (3H, s), 1.99 (3H, s), 1.91–1.86 (1H, m), 1.80–1.55 (11 H, m), 1.52-1.36 (3H, m), 1.31-1.12 (6H, m), 1.00 (3H, d, I = 7.0 Hz), 0.83 (3H, s), 0.79 (3H, d, J = 6.3 Hz); $^{13}\text{C}\{^1\text{H}\}\text{NMR}$ (100 MHz, $CDCl_3$) δ 180.2, 170.1, 159.6, 144.8, 135.3, 129.4, 128.7, 116.9, 109.2, 80.5, 77.2, 72.4, 66.8, 61.1, 49.7, 48.7, 41.5, 40.8, 40.1, 39.1, 38.2, 38.1, 36.0, 34.7, 31.4, 30.2, 28.8, 27.2, 24.3, 21.7, 21.2, 20.5, 17.5, 17.1, 16.6, 14.7; HRMS (ESI-Orbitrap) m/z [M + H]⁺ calcd for C₃₈H₅₃O₇N₂S⁺ 681.3574, found 681.3565.

Compound 9. Steps 1-3 were performed identically to those for the synthesis for compound 4. The hydrazone of cholesterol (0.83 g, 1.36 mmol) was then dissolved in anhydrous THF (20 mL), and to the solution were added K₂CO₃ (0.3 g, 2.17 mmol, 1.6 equiv) and PPh₃ (96 mg, 0.36 mmol, 0.27 equiv). Methyl iodide (0.17 mL, 2.72 mmol, 2.0 equiv) was added dropwise, and the mixture was stirred at room temperature for 36 h. The reaction was quenched with water, transferred to a separatory funnel, and extracted with Et₂O (3×). The combined organic layers were washed with brine, dried over Na₂SO₄, and concentrated to dryness. Purification via column chromatography on silica gel (EtOAc/hexanes) provided compound 9 as a white solid (0.67 g, 79%): 1 H NMR (400 MHz, CDCl₃) δ 7.76–7.73 (2H, m), 7.32-7.29 (2H, m), 6.61 (1H, d, J = 1.6 Hz), 4.73-4.64 (1H, m), 2.67 (3H, s), 2.59-2.52 (1H, m), 2.50-2.35 (5H, m), 2.32-2.23 (1H, m), 2.05 (3H, s), 2.03-1.87 (3H, m), 1.77-1.68 (1H, m), 1.59-1.49 (3H, m), 1.39-1.25 (6H, m), 1.18-1.04 (10H, m), 0.92 (3H, d, J = 6.6 Hz), 0.89-0.87 (6H, m), 0.86-0.76 (2H, m), 0.68(3H, s); ${}^{13}C\{{}^{1}H\}NMR$ (100 MHz, CDCl₃) δ 174.7, 170.3, 156.5, 143.7, 131.2, 129.7, 128.9, 117.0, 72.7, 54.7, 50.0, 49.1, 42.8, 40.0, 39.5, 39.4, 38.7, 38.3, 38.0, 36.2, 36.2, 35.6, 28.2, 28.0, 27.4, 26.9, 23.7, 22.8, 22.6, 21.6, 21.3, 20.7, 18.9, 17.5, 12.2; HRMS (ESI-Orbitrap) m/z [M + H]⁺ calcd for $C_{37}H_{57}O_4N_2S^+$ 625.4040, found 625.4033.

COMPUTATIONAL METHODS

Density functional theory calculations were performed using the software package Gaussian 09, rev. E.01.²⁸ All geometry optimizations were performed applying the ω B97X-D²⁹ functional with the 6-31G(d,p) basis set. The optimized geometries were verified as transition state structures (one imaginary frequency) or minima by frequency calculations. Intrinsic reaction coordinate (IRC) calculations³⁰ were performed to confirm that all transition state structures were linked to the relevant minima. The energies of the ω B97X-D/6-31G(d,p)-optimized structures were further refined by single-point calculations performed at the ω B97X-D/6-311+G(d,p) level of theory using the integral equation formalism polarizable continuum model (IEFPCM) with the default parameters of acetonitrile ($\varepsilon = 37.5$) to account for solvent.³¹ The final reported Gibbs free energies were the summed thermal corrections to the Gibbs free energies (T = 298.15K) computed at the lower (ω B97X-D/6-31G(d,p)) level of theory and electronic energies from the single-point ω B97X-D/6-311+G-(d,p) calculations. The keyword (integral = grid = ultrafine) was used for all calculations. The 3D images of all optimized geometries were generated with CYLview, 32 and GaussView 33 was used to construct all structures prior to optimization as well as visualize the output from the Gaussian 09 calculations. Monte Carlo conformational searches (MCCS) with an OPLS3 force field were performed using the MacroModel program of the Schrödinger software package. reported molecular electrostatic potential (MEP) surfaces (isovalue = 0.001, min = 50.0, and max = 110.0) were computed using the B3LYP-D3 functional with a 6-311+G(d,p) basis set using the Jaguar program in the Schrödinger software package.³

ASSOCIATED CONTENT

5 Supporting Information

The Supporting Information is available free of charge at https://pubs.acs.org/doi/10.1021/acs.joc.0c02716.

NMR spectral data of fluorinated products, NMR spectral data of starting materials, structure and properties of compound 9, and single-crystal X-ray crystallography and computational data (PDF)

FAIR data, including the primary NMR FID files, for compounds 2–9 (ZIP)

Accession Codes

CCDC 2041353 contains the supplementary crystallographic data for this paper. These data can be obtained free of charge via www.ccdc.cam.ac.uk/data_request/cif, or by emailing data_request@ccdc.cam.ac.uk, or by contacting The Cambridge Crystallographic Data Centre, 12 Union Road, Cambridge CB2 1EZ, UK; fax: +44 1223 336033.

AUTHOR INFORMATION

Corresponding Authors

Thomas Lectka — Department of Chemistry, Johns Hopkins University, Baltimore, Maryland 21218, United States; orcid.org/0000-0003-3088-6714; Email: lectka@jhu.edu

Travis Dudding — Department of Chemistry, Brock University, St. Catharines, ON L2S 3A1, Canada; orcid.org/0000-0002-2239-0818; Email: tdudding@brocku.ca

Authors

Joseph N. Capilato – Department of Chemistry, Johns Hopkins University, Baltimore, Maryland 21218, United States; oorcid.org/0000-0001-5996-2456

Maxime A. Siegler — Department of Chemistry, Johns Hopkins University, Baltimore, Maryland 21218, United States; orcid.org/0000-0003-4165-7810

Rozhin Rowshanpour – Department of Chemistry, Brock University, St. Catharines, ON L2S 3A1, Canada

Complete contact information is available at: https://pubs.acs.org/10.1021/acs.joc.0c02716

Notes

The authors declare no competing financial interest.

ACKNOWLEDGMENTS

T.L. thanks the National Science Foundation (CHE 1800510) for support. The authors also thank the Mass Spectrometry Facility at the University of Delaware. T.D. acknowledges financial support from the Natural Science and Engineering Research Council (NSERC) Discovery Grant (2019-04205). Computations were carried out using facilities at SHARCNET (Shared Hierarchical Academic Research Computing Network, www.sharcnet.ca) and Compute/Calcul Canada.

REFERENCES

- (1) (a) Desiraju, G. R.; Steiner, T. The Weak Hydrogen Bond In Structural Chemistry and Biology; Oxford University Press, Inc.: New York, NY, 2001. (b) Nishio, M.; Umezawa, Y.; Fantini, J.; Weiss, M. S.; Chakrabarti, P. $CH-\pi$ hydrogen bonds in biological macromolecules. Phys. Chem. Chem. Phys. **2014**, 16, 12648–12683.
- (2) Yeagle, P. L. The Structure of Biological Membranes, 2nd ed.; CRC Press: Boca Raton, FL, 2004.
- (3) Hanson, M. A.; Cherezov, V.; Griffith, M. T.; Roth, C. B.; Jaakola, V. P.; Chien, E. Y.; Velasquez, J.; Kuhn, P.; Stevens, R. C. A Specific Cholesterol Binding Site Is Established by the 2.8 Å Structure of the Human β 2-Adrenergic Receptor. *Structure* **2008**, *16*, 897–905.
- (4) (a) Pitts, C. R.; Bume, D. D.; Harry, S. A.; Siegler, M. A.; Lectka, T. Multiple enone-directed reactivity modes lead to the selective photochemical fluorination of polycyclic terpenoid derivatives. *J. Am. Chem. Soc.* **2017**, *139*, 2208–2211. (b) Bume, D. D.; Harry, S. A.; Pitts, C. R.; Lectka, T. Sensitized aliphatic fluorination directed by terpenoidal enones: A "visible light" approach. *J. Org. Chem.* **2018**, *83*, 1565–1575. (c) Capilato, J. N.; Bume, D. D.; Lee, W. H.; Hoffenberg, L. E. S.; Jokhai, R. T.; Lectka, T. Fluorofunctionalization of C= C Bonds with Selectfluor: Synthesis of β -Fluoropiperazines through a Substrate-Guided Reactivity Switch. *J. Org. Chem.* **2018**, *83*, 14234–14244. (d) Capilato, J. N.; Pitts, C. R.; Rowshanpour, R.; Dudding, T.; Lectka, T. Site-Selective Photochemical Fluorination of Ketals: Unanticipated Outcomes in Selectivity and Stability. *J. Org. Chem.* **2020**, *85*, 2855–2864.
- (5) Eberling, P.; Koivisto, V. A. Physiological importance of dehydroepiandrosterone. *Lancet* **1994**, *343*, 1479–1481.
- (6) (a) Numazawa, M.; Mutsumi, A.; Tachibana, M.; Hoshi, K. Synthesis of androst-5-en-7-ones and androsta-3, 5-dien-7-ones and their related 7-deoxy analogs as conformational and catalytic probes for the active site of aromatase. *J. Med. Chem.* **1994**, *37*, 2198–2205. (b) Arsenou, E. S.; Fousteris, M. A.; Koutsourea, A. I.; Papageorgiou, A.; Karayianni, V.; Mioglou, E.; Iakovidou, Z.; Mourelatos, D.; Nikolaropoulos, S. S. The allylic 7-ketone at the steroidal skeleton is crucial for the antileukemic potency of chlorambucil's active metabolite steroidal esters. *Anti-Cancer Drugs* **2004**, *15*, 983–990.
- (7) Friščić, T.; Lancaster, R. W.; Fabian, L.; Karamertzanis, P. G. Tunable recognition of the steroid α -face by adjacent π -electron density. *Proc. Natl. Acad. Sci. U. S. A.* **2010**, *107*, 13216–13221.
- (8) Bume, D. D.; Pitts, C. R.; Ghorbani, F.; Harry, S. A.; Capilato, J. N.; Siegler, M. A.; Lectka, T. Ketones as directing groups in photocatalytic sp³ C–H fluorination. *Chem. Sci.* **2017**, *8*, 6918–6923.
- (9) It should be noted that the hydrogen atoms were placed at calculated positions; thus, the C_6 -H distance was fixed. The C_6 -N distance was measured to be 2.72 Å.
- (10) Nishio, M.; Umezawa, Y.; Honda, K.; Tsuboyama, S.; Suezawa, H. CH/π hydrogen bonds in organic and organometallic chemistry. CrystEngComm 2009, 11, 1757–1788.

- (11) Lam, Y. P.; Yeung, Y. Y. Metal-Free Allylic Oxidation of Steroids Using TBAI/TBHP Organocatalytic Protocol. *Chem. Asian J.* **2018**, *13*, 2369–2372.
- (12) Stork, G.; Brizzolara, A.; Landesman, H.; Szmuszkovicz, J.; Terrell, R. The enamine alkylation and acylation of carbonyl compounds. *J. Am. Chem. Soc.* **1963**, 85, 207–222.
- (13) (a) Charaschanya, M.; Aubé, J. Reagent-controlled regiodivergent ring expansions of steroids. *Nat. Commun.* **2018**, *9*, 943. (b) Szendi, Z.; Dombi, G.; Vincze, I. Steroids, LIII: New routes to aminosteroids. *Monatsh. Chem.* **1996**, 127, 1189–1196.
- (14) Spectroscopic evidence of the C-H interaction was observed for this steroid; while the vinylic hydrogen atom was significantly deshielded compared to that of 4h (6.61 vs 5.98 ppm), the signal was sharp rather than broad (see the Supporting Information).
- (15) To rationalize this finding, we propose that the electron-withdrawing imide moiety facilitates the tautomerization of the α,β -unsaturated hydrazone to the reactive conjugated dienamine.
- (16) Jasem, Y. A.; Thiemann, T.; Gano, L.; Oliveira, M. C. Fluorinated steroids and their derivatives. *J. Fluorine Chem.* **2016**, *185*, 48–85.
- (17) (a) Hutchins, R. O.; Milewski, C. A.; Maryanoff, B. E. Selective deoxygenation of ketones and aldehydes including hindered systems with sodium cyanoborohydride. *J. Am. Chem. Soc.* **1973**, *95*, 3662–3668. (b) Caglioti, L.; Magi, M. The reaction of tosylhydrazones with lithium aluminium hydride. *Tetrahedron* **1963**, *19*, 1127–1131.
- (18) Although we employed freshly dried or distilled solvent for the reaction, evidently a trace quantity of water was still present in the reaction. Given the typical acid-catalyzed mechanism for hydrazone hydrolysis, we propose that Selectfluor fluorinates the hydrazone nitrogen atom, initiating the hydrolysis.
- (19) Salvador, J.A.R.; Sae Melo, M.L.; Campos Neves, A.S. Coppercatalysed allylic oxidation of ΔS -steroids by t-butyl hydroperoxide. *Tetrahedron Lett.* **1997**, 38, 119–122.
- (20) Mourelatos, C.; Kareli, D.; Dafa, E.; Argyraki, M.; Koutsourea, A.; Papakonstantinou, I.; Fousteris, M.; Pairas, G.; Nikolaropoulos, S.; Lialiaris, T. S. Cytogenetic and antineoplastic effects by newly synthesised steroidal alkylators in lymphocytic leukaemia P388 cells in vivo. *Mutat. Res., Genet. Toxicol. Environ. Mutagen.* 2012, 746, 1–6.
- (21) Moalic, S.; Liagre, B.; Corbière, C.; Bianchi, A.; Dauça, M.; Bordji, K.; Beneytout, J. L. A plant steroid, diosgenin, induces apoptosis, cell cycle arrest and COX activity in osteosarcoma cells. *FEBS Lett.* **2001**, *506*, 225–230.
- (22) Rozatian, N.; Harsanyi, A.; Murray, B. J.; Hampton, A. S.; Chin, E. J.; Cook, A. S.; Hodgson, D. R.; Sandford, G. Kinetics of electrophilic fluorination of steroids and epimerisation of fluorosteroids. *Chem. Eur. J.* **2020**, *26*, 12027–12035.
- (23) Poss, A. J.; Shia, G. A. γ-Fluorination of Unsaturated Ketones with N-Fluorobenzenesulfonimide. *Tetrahedron Lett.* **1995**, *36*, 4721–4724
- (24) Ghorbani, F.; Harry, S. A.; Capilato, J. N.; Pitts, C. R.; Joram, J.; Peters, G. N.; Tovar, J. D.; Smajlagic, I.; Siegler, M. A.; Dudding, T.; Lectka, T. Carbonyl-Directed Aliphatic Fluorination: A Special Type of Hydrogen Atom Transfer Beats Out Norrish II. *J. Am. Chem. Soc.* **2020**, *142*, 14710–14724.
- (25) Wood, S. H.; Etridge, S.; Kennedy, A. R.; Percy, J. M.; Nelson, D. J. The Electrophilic Fluorination of Enol Esters Using SelectFluor: A Polar Two-Electron Process. *Chem. Eur. J.* **2019**, *25*, 5574–5585.
- (26) The sulfonyl two-point hydrogen bond in α -TS1 $_{\alpha}$ is not present in α -TS1 $_{\beta}$. Instead, a bifurcated hydrogen bond arrangement with distances of 2.22 and 2.27 Å was observed, representing a potential source of destabilization and making α -TS1 β disfavored (see the Supporting Information).
- (27) Taylor, S. D.; Kotoris, C. C.; Hum, G. Recent advances in electrophilic fluorination. *Tetrahedron* **1999**, *55*, 12431–12477.
- (28) Frisch, M. J.; Trucks, G. W.; Schlegel, H. B.; Scuseria, G. E.; Robb, M. A.; Cheeseman, J. R.; Scalmani, G.; Barone, V.; Mennucci, B.; Petersson, G. A.; Nakatsuji, H.; Caricato, M.; Li, X.; Hratchian, H. P.; Izmaylov, A. F.; Bloino, J.; Zhang, G.; Sonnenberg, J. L.; Hada, M.; Ehara, M.; Toyota, K.; Fukuda, R.; Hasegawa, J.; Ishida, M.;

- Nakajima, T.; Honda, Y.; Kitao, O.; Nakai, H.; Vreven, T.; Montgomery, J. A., Jr.; Peralta, J. E.; Ogliaro, F.; Bearpark, M.; Heyd, J. J.; Brothers, E.; Kudin, K. N.; Staroverov, V. N.; Kobayashi, R.; Normand, J.; Raghavachari, K.; Rendell, A.; Burant, J. C.; Iyengar, S. S.; Tomasi, J.; Cossi, M.; Rega, N.; Millam, J. M.; Klene, M.; Knox, J.e.; Cross, J. B.; Bakken, V.; Adamo, C.; Jaramillo, J.; Gomperts, R.; Stratmann, R. E.; Yazyev, O.; Austin, A. J.; Cammi, A. R.; Pomelli, C.; Ochterski, J. W.; Martin, R. L.; Morokuma, K.; Zakrzewski, V. G.; Voth, G. A.; Salvador, P.; Dannenberg, J. J.; Dapprich, S.; Daniels, A. D.; Farkas, Ö.; Foresman, J. B.; Ortiz, J. V.; Cioslowski, J.; Fox, D. J. Gaussian 09, rev. E.01; Gaussian, Inc.: Wallingford, CT, 2009.
- (29) Chai, J.-D.; Head-Gordon, M. Long-range corrected hybrid density functionals with damped atom—atom dispersion corrections. *Phys. Chem. Phys.* **2008**, *10*, 6615—6620.
- (30) (a) González, C.; Schlegel, H. B. Reaction path following in mass-weighted internal coordinates. *J. Phys. Chem.* **1990**, *94*, 5523–5527. (b) Fukui, K. The Path of Chemical Reactions The IRC Approach. *Acc. Chem. Res.* **1981**, *14*, 363–368.
- (31) Cancès, E.; Mennucci, B.; Tomasi, J. A New Integral Equation Formalism for the Polarizable Continuum Model: Theoretical Background and Applications to Isotropic and Anisotropic Dielectrics. *J. Chem. Phys.* **1997**, *107*, 3032–3041.
- (32) Legault, C. Y. CYLview, ver. 1.0b; Universite de Sherbrooke: Quebec, Canada, 2009. http://www.cylview.org.
- (33) Dennington, R.; Keith, T.; Millam, J. GaussView, ver. 5; Semichem, Inc.: Shawnee, KS, 2009.
- (34) Schrödinger Release 2019-2: MacroModel; Schrödinger, LLC: New York, NY, 2019.
- (35) Schrödinger Release 2019-2: Jaguar; Schrödinger, LLC: New York, NY, 2019.